Peripapillary and Macular Vessel Density Measurement With Optical Coherence Tomography Angiography in Exfoliation Syndrome

Sirel Gür Güngör, MD, Almila Sarıgül Sezenöz, MD, FEBO, Caner Öztürk, MD, Gülşah Gökgöz, MD, and Ahmet Akman, MD

Precis: Although peripapillary retinal nerve fiber layer thickness (RNFLTs) and vessel density (VD) values were similar to healthy group, eyes with exfoliation syndrome had significantly lower superficial macular VDs and minimum ganglion cell analysis values.

Purpose: To compare peripapillary and macular perfused capillary densities with optical coherence tomography angiography (OCT-A) between patients with eyes having exfoliation syndrome (XFS) and normal age-matched healthy controls.

Patients and Methods: This cross-sectional study included patients diagnosed with XFS from December 2017 to January 2020 at the Glaucoma Department. Peripapillary and parafoveal superficial VDs were obtained using OCT-A. The RNFLTs and ganglion cell analysis values were compared.

Results: Thirty-nine eyes of 39 XFS patients (26 women; mean age, 69.0 ± 8.1 y) and 39 eyes of 39 healthy patients (25 women; mean age, 68.0 ± 8.6 y) were enrolled. There were no statistically significant differences in sex or age distribution, central corneal thickness measurements, refractive errors, or intraocular pressures between both groups (all $P > 0.05$). There were no statistically significant differences in the peripapillary VD or peripapillary RNFLT between XFS eyes and healthy eyes ($P > 0.05$ for all). In the macular region, most superficial VD parameters were significantly reduced in the XFS group ($P = 0.02$ for parafoveal VD, $P = 0.04$ for both hemifields). While the average ganglion cell and internal plexiform layer (GCL+IPL) values were similar between groups ($P = 0.19$), the minimum GCL+IPL value was lower in the XFS group than in the healthy group ($P = 0.03$).

Conclusion: Although structural test results, especially peripapillary RNFLT and mean GCL+IPL, were similar between the healthy and XFS groups, macular VD values were lower in XFS eyes. Our findings implicate microvascular damage can be the mechanism underlying XFS-related changes and indicate that it precedes significant structural damage.

Key Words: optical coherence tomography angiography, exfoliation syndrome, retinal nerve fiber layer thicknesses, vessel density

(*J Glaucoma* 2021;30:71–77)

With a global prevalence of ~60 million, exfoliation syndrome (XFS) is an age-related systemic disorder characterized by abnormal extracellular fibrillary material deposition that induces basement membrane damage and degenerative cellular changes and a wide range of ocular pathologies.[1–5] The most common complications of XFS in the eye include glaucoma, cataract, phacodonesis and zonulopathy, angle closure, and retinal venous occlusive diseases.[3]

Several studies have linked XFS to various systemic vascular abnormalities.[6–9] Exfoliative material found to be present in the walls of short posterior ciliary arteries and vortex veins have been implicated in disturbances in the microvascular blood flow of the optic nerve head and peripapillary retina.[10,11] XFS has also been associated with iris vasculopathy, as indicated by the degeneration of smooth muscle cells, pericytes, and endothelial cells; abnormalities of the endothelial basement membrane; and obliteration of the vascular lumen.[12–14]

The recent advent of optical coherence tomography angiography (OCT-A) allows for the rapid noninvasive assessment of the microvasculature in various retinal and choroid layers.[15] Developed to improve the performance of OCT-A, the split-spectrum amplitude-decorrelation angiography (SSADA) algorithm detects the movement of red blood cells within retinal and choroidal vessels to rapidly, reliably, and noninvasively generate angiographic images of perfused vessels in both the perifoveal and peripapillary regions.[16]

Prior studies using OCT-A reported the progressive decrease of peripapillary perfused capillary density from XFS syndrome, through primary open-angle glaucoma (POAG), to XFS glaucoma.[17] However, no study has evaluated both the peripapillary and macular vessel density (VD) parameter changes in XFS. Vascular changes in the peripapillary and macular region may contribute to XFS pathogenesis. This study aimed to compare peripapillary and macular VDs with OCT-A between patients with eyes having XFS and normal age-matched healthy controls.

PATIENTS AND METHODS

This cross-sectional study was performed at a tertiary hospital, was approved by the local ethics committee (KA18/262), and adhered to the tenets of the Declaration of Helsinki. We recruited patients with XFS examined at the glaucoma department of Başkent University from December 2017 to January 2020. Written informed consent was obtained from all subjects to participate in this study. All patients underwent comprehensive ophthalmologic examinations, including the measurement of the best-corrected visual acuity (BCVA), slit-lamp biomicroscopy, the assessment of intraocular pressure (IOP) with Goldmann applanation tonometry, gonioscopy, ultrasound pachymetry, color fundus photography, standard automated perimetry, OCT, and OCT-A.

Received for publication May 8, 2020; accepted September 12, 2020.
From the Department of Ophthalmology, Faculty of Medicine, Başkent University, Ankara, Turkey.
Disclosure: The authors declare no conflict of interest.
Reprints: Sirel Gür Güngör, MD, Faculty of Medicine, Baskent University, Fevzi Çakmak Caddesi, Bahçelievler, Ankara 06490, Turkey (e-mail: sirelgur@yahoo.com).

DOI: 10.1097/IJG.0000000000001685

Included XFS eyes were required to exhibit exfoliation material on the lens, as revealed by biomicroscopic evaluation; a normal-appearing optic nerve; a lack of glaucomatous damage on both peripapillary and macular OCT; and normal perimetry. While selecting patients with XFS, caution was exercised to avoid glaucoma in both eyes. Enrolled healthy eyes had an IOP <21 mm Hg with no history of elevated IOP; absence of exfoliation material; normal-appearing optic disc on clinical examination; normal peripapillary and macular OCT; and no visual field defects. Gonioscopy was also performed on all healthy eyes to exclude angle-only signs of XFS. The criteria required for all eyes were as follows: no evidence of retinal pathology, ocular media opacity, significant refractive error (myopia of 3 D or hyperopia of 3 D or more), or chronic ocular or systemic corticosteroid use; an open anterior chamber angle on gonioscopy; a retinal nerve fiber layer thickness (RNFLT) measured on OCT within the 95% confidence interval of the normal distribution; and no visual field defects on 24-2 SITA standard tests. All patients had a BCVA of at least 20/25 and were 20 years of age or older. Exclusion criteria included glaucoma, diabetes mellitus, hypertension, other ocular conditions, and a history of intraocular surgery.

The OCT-A images were obtained using the 2017.1.0.151 version of the RTVue XR Avanti device (Avanti RTVue-XR; Optovue, Fremont, CA), which can perform 70000 A-mode scans per second using a light source centered on a 840-nm light. The SSADA algorithm improves the image quality yielded by this device, as well as its scanning time. The algorithm distinguishes the movement of red blood cells within the lumen of retinal and choroidal vessels between cross-sectional scans. The decorrelation algorithm identifies perfused retinal vessel from surrounding static tissue based upon signal amplitude variation differences in nonstatic tissue relative to static tissue.[18] The segmentation of the vascular structures in the scanned areas was automatically performed with the built-in AngioVue software. The macula OCT-A scans were obtained in a 6×6-mm area and disc OCT-A scans were obtained in a 4.5×4.5-mm area. Measurements with a signal strength $\geq$6/10 were considered suitable for analysis. Patients whose images featured inadequate signal strength or artifacts were excluded.

The parameters evaluated from the disc OCT-A images included whole-image peripapillary VD (WI-PPVD); peripapillary VD (PPVD); superior hemisphere peripapillary VD (SH-PPVD); inferior hemisphere peripapillary VD (IH-PPVD); and nasal, inferior, temporal, and superior peripapillary VDs (N-PPVD, I-PPVD, T-PPVD, and S-PPVD, respectively).

The parameters evaluated with the macula OCT-A included whole-image macular VD (WI-MVD); parafoveal VD (PFVD); inferior hemisphere parafoveal VD (IH-PVVD); superior hemisphere parafoveal VD (SH-PFVD); and nasal, inferior, temporal, and superior parafoveal VDs (N-PFVD, I-PFVD, T-PFVD, and S-PFVD, respectively). Vessel density was reported as the percentage of the total area occupied by blood vessels. To calculate VD, AngioVue Analytics extracts a binary image of the blood vessels from the gray scale OCT-A image and then calculates the percentage of pixels occupied by blood vessels in the defined region.[19]

The OCT-A of the optic disc was performed in a 4.5×4.5-mm area around the optic disc. The optic disc VDs were automatically obtained. The instrument uses rings with diameters of 2 and 4 mm centered on the optic disc. The area within the circle with a 2 mm diameter was evaluated as the intrapapillary region, while that between the inner 2 mm diameter ring and the outer 4 mm diameter ring was defined as the peripapillary region. The WI-PPVD was obtained from the 4.5×4.5-mm area. Using OCT-A, both the VD of the radial peripapillary capillary (RPC) network and the total VD of the large vessels with the capillary network could be calculated. The OCT-A device takes into account the VD of the region between the internal limiting membrane and the outer border of the RNFL when calculating the RPC network. The RNFL vascular network was examined using capillary VD values.

The RTVue XR Avanti device was used to perform macular evaluation in an area of 6×6 mm. The superficial capillary plexus is important for nourishing the ganglion cell layer. An area delineated by the internal limiting membrane as the inner boundary and the inner plexiform layer offset inwards by 10 μm as the outer boundary was automatically created by the OCT-A device to evaluate the superficial capillary plexus. Anatomic structures are defined by 3 intertwined rings centered on the fovea. The innermost circle with a 1-mm diameter represents the fovea. The annulus between the 3-mm diameter ring in the middle and innermost ring with a 1-mm diameter represents the parafoveal region. The annulus between the outermost ring with a 6-mm diameter and the middle ring of a 3-mm diameter represents the perifoveal region. The WI-MVD was calculated in the 6×6-mm area around the fovea. We examined the VDs of the parafoveal region, where ganglion cells are found in the greatest density, and the superficial capillary plexus, which is responsible for nourishing the ganglion cells.

OCT scanning of the patients participating in the study was performed with Cirrus HD Spectral Domain OCT (Carl Zeiss Meditec, Dublin, CA). This device was used to obtain the optic nerve cupping to optic disc ratio, disc area, rim area, mean RNFLT, superior RNFLT (S-RNFLT), inferior RNFLT (I-RNFLT), nasal RNFLT (N-RNFLT), and temporal RNFLT (T-RNFLT). In addition, the macular ganglion cell analysis (GCA) measurements were collected with this device. Measurements with a signal strength $\geq$6/10 were considered suitable for analysis. GCA measurements were performed with the automatic segmentation feature of the OCT device. The ganglion cell layer and internal plexiform layer thickness (GCL+IPL) were taken into consideration. The minimum, mean, and sectoral GCL+IPL thickness measurements were evaluated. The GCA algorithm calculates the mean GCL+IPL thickness by 1 degree interval of the 360 spokes of the elliptical annulus using data set from 50 to 60 sampling points and the lowest measurement thus obtained was defined as the minimum GCL+IPL thickness.[20] The topographic relationship of sectoral GCL+IPL thicknesses with sectoral parafoveal VDs was assessed. Figures 1 and 2 present the OCT and OCT-A images of representative healthy and XFS cases, respectively (Figs. 1, 2).

Visual field examinations were performed using the Humphrey Visual Field Analyzer Humphrey Instruments Model 740 (Carl Zeiss Meditec, Dublin, CA) and the 24-2 SITA standard program. IOP's were measured using the Goldmann applanation tonometry method with fluorescein under topical anesthesia. Goldmann applanation tonometry was performed using a slit lamp (Takagi slit-lamp microscope SM-70N, Takagi Inc., Manchester, UK) mounted on a Goldmann tonometer. All measurements were obtained by a glaucoma specialist (S.G.G) between 8.30 and 10.30 AM. Each metric was measured at least twice in each eye.

The IBM Statistics Package for the Social Sciences version 25.0 (SPSS version 25.0) statistics program was used for data analysis. The Mann-Whitney *U* test and independent

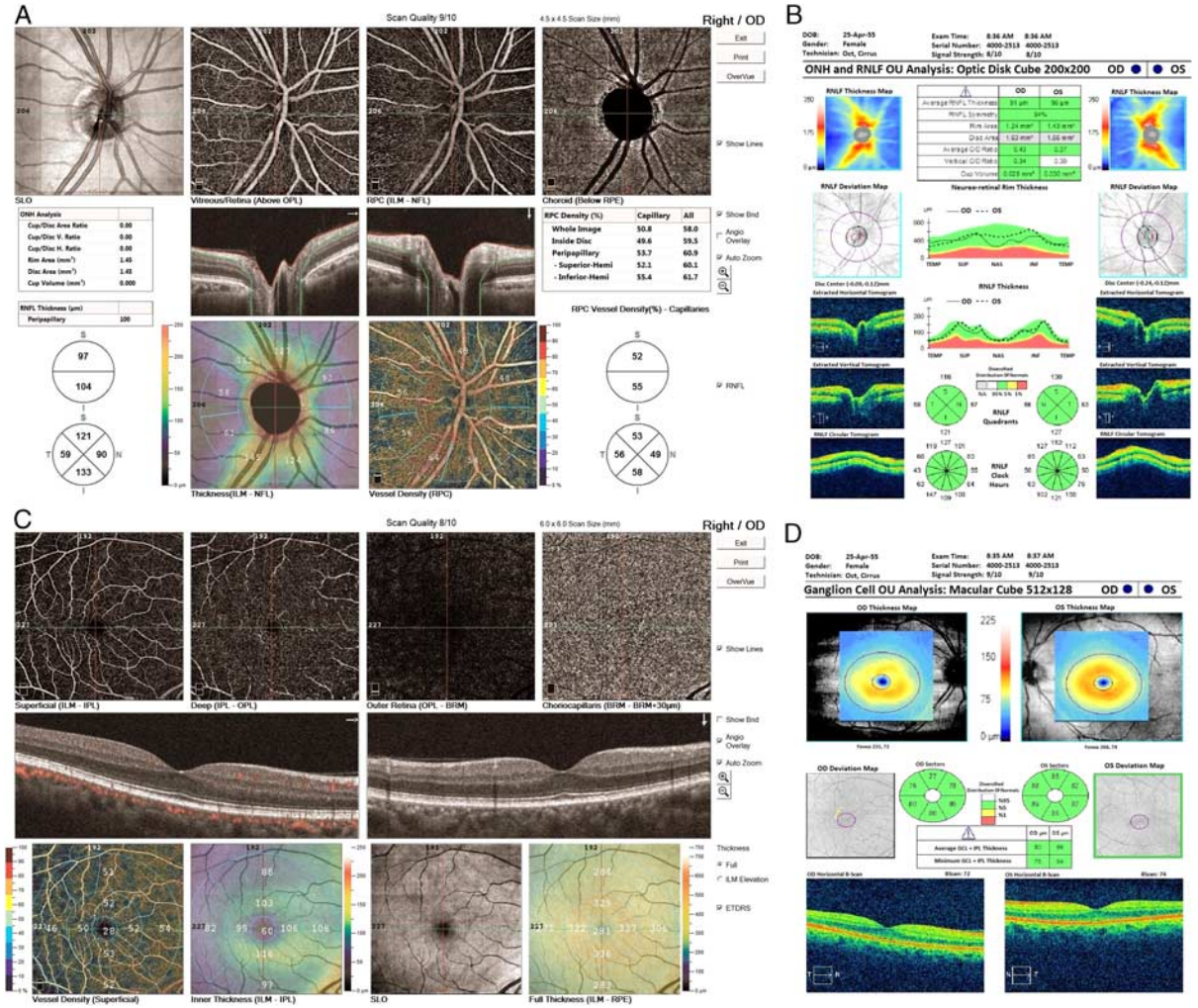

FIGURE 1. Optical coherence tomography (OCT) and optical coherence tomography angiography (OCT-A) images of a healthy patient. A, Peripapillary OCT-A. B, Peripapillary OCT. C, Macular OCT-A. D, Macular OCT. Figure 1 can be viewed in color online at www.glaucomajournal.com.

t test were used to compare nonparametric and normally distributed data, respectively. Spearman correlation test was used to assess the correlation between measurements. *P*-values <0.05 were considered to indicate statistical significance.

RESULTS

Thirty-nine eyes of 39 XFS patients (26 women, 13 men) and 39 eyes of 39 healthy controls (25 women, 14 men) were enrolled. The mean ages were 69.0 ± 8.1 and 68.0 ± 8.6 years in the XFS and healthy groups, respectively ($P = 0.57$). The demographic and clinical characteristics of the study participants are presented in Table 1. There were no statistically significant differences between the groups in terms of sex or age distribution, central corneal thickness measurements, refractive errors, or IOPs (all $P > 0.05$).

Although the RNFLT values of the XFS group were lower than those of the healthy group in all quadrants, this difference was not significant ($P > 0.05$). The peripapillary RNFLT measurements of the groups are shown in Table 2. Other disc parameters measured using OCT were also found to be similar between the 2 groups ($P > 0.05$; Table 3).

GCL+IPL thickness values were obtained with GCA (Table 2). Mean GCL+IPL thicknesses were similar between the groups ($P = 0.19$). However, the minimum GCL+IPL thickness of XFS eyes was significantly thinner than that of healthy eyes ($P = 0.03$). Analyzed according to sector, the difference was found to be significant in the superior, superior nasal, inferior nasal, and inferior segments ($P = 0.01$, <0.01, 0.01, 0.03, respectively; Table 2).

The peripapillary VDs were similar between the two groups. Although peripapillary VD values of the XFS group were lower than those of the healthy group in all quadrants, the difference was not statistically significant ($P > 0.05$). Peripapillary VD values are shown in Table 4.

Unlike peripapillary VD values, most macular VD values were lower in the XFS group (Table 5). The PFVD, SH-PFVD, IH-PFVD, T-PFVD, and N-PFVD values of XFS eyes were lower than those of healthy eyes ($P = 0.02$, 0,04, 0.04, 0.04, and 0.01, respectively). Superior hemi (SH)

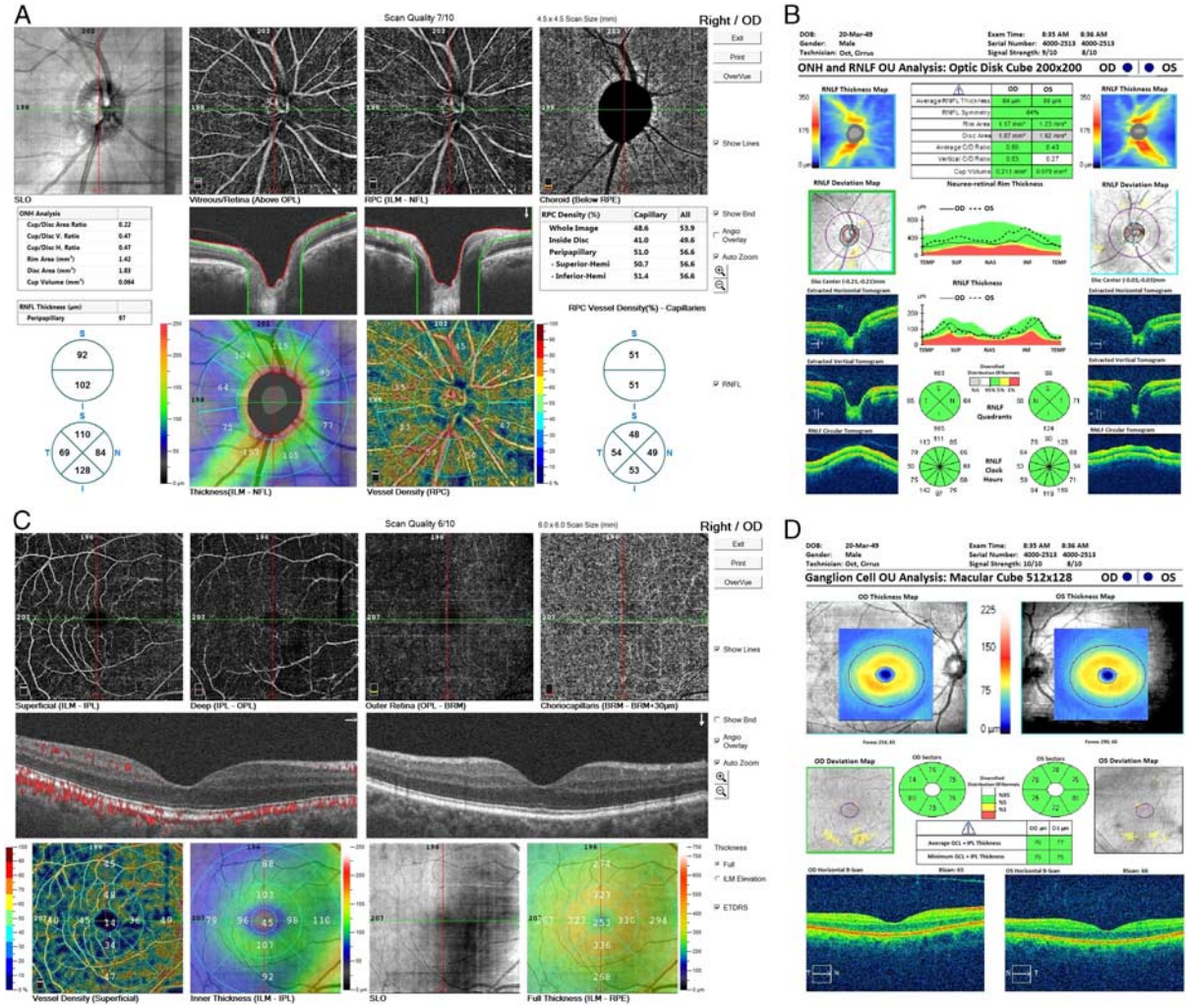

FIGURE 2. Optical coherence tomography (OCT) and optical coherence tomography angiography (OCT-A) images of a patient with exfoliation syndrome. A, Peripapillary OCT-A. B, Peripapillary OCT. C, Macular OCT-A. D, Macular OCT. Figure 2 can be viewed in color online at www.glaucomajournal.com.

GCL+IPL and inferior hemi (IH) GCL+IPL were calculated as the arithmetic sum of the GCL+IPL quadrant values in the same hemisphere to examine the correlation between SH PFVD and IH PFVD values. When the correlation between the superior and inferior hemi GCL+IPL and the PFVD values of the corresponding macular region was investigated, no significant relationship was observed. However, a correlation was found between the mean GCL+IPL and both WI-MVD and PFVD in XFS eyes ($r = 0.432$, $P < 0.01$ and $r = 0.296$, $P = 0.04$, respectively). Similarly, we found a correlation between the minimum GCL+IPL and both WI-MVD and PFVD in these eyes ($r = 0.422$, $P < 0.01$ and $r = 0.302$, $P = 0.04$, respectively) (Table 6).

TABLE 1. Age, Intraocular Pressure, Visual Acuity, Spherical Equivalent and Gender Characteristics of the Groups

	Healthy	XFS	P*
Age (y)	68.0 ± 8.6	69.0 ± 8.1	0.57
Intraocular pressure (mm Hg)	15.8 ± 0.5	14.4 ± 0.4	0.63
Visual acuity (Snellen)	0.95 ± 0.19	0.96 ± 0.14	0.52
Spherical equivalent (D)	−0.18 ± 0.16	−0.27 ± 0.18	0.27
Sex (M/F)	14/25	13/26	0.27
Central corneal thickness (μm)	556.17 ± 17.52	550.22 ± 23.15	0.67

Comparisons with significance level $P < 0.05$ were considered statistically significant.

*The average comparison test between nonparametric groups was analyzed by Mann-Whitney U test (Healthy vs. XFS).

F indicates female; M, male; XFS, Exfoliation syndrome.

DISCUSSION

Our study demonstrated decreased macular VDs in eyes with XFS whose peripapillary VDs, RNFLT and the mean GCL+IPL thickness values were similar to healthy eyes (Figs. 1, 2). We further found that minimum GCL+IPL and sectoral GCL+IPL values in these XFS eyes were also diminished and there was a correlation between GCL+IPL thickness and macular VDs. Although longitudinal prospective studies are needed to determine whether vascular change precedes axonal loss, our results support the hypothesis that

Copyright © 2020 Wolters Kluwer Health, Inc. All rights reserved.

TABLE 2. RNFLT and GCL+IPL Measurements of the Groups Measured by OCT

	Healthy	XFS	*P**
Mean RNFLT, μm	101.21 ± 16.88	99.03 ± 9.43	0.10
Superior RNFLT, μm	117.24 ± 25.92	116.03 ± 17.51	0.53
Temporal RNFLT, μm	75.14 ± 7.66	73.72 ± 14.94	0.42
Inferior RNFLT, μm	125.71 ± 32.77	120.05 ± 15.18	0.24
Nasal RNFLT, μm	80.50 ± 17.64	79.62 ± 13.72	0.41
Average GCL+IPL, μm	78.92 ± 6.12	76.32 ± 8.63	0.19
Minimum GCL+IPL, μm	76.16 ± 7.43	70.54 ± 13.46	**0.03**
Superior temporal GCL +IPL, μm	79.12 ± 6.28	76.71 ± 9.19	0.27
Superior GCL+IPL, μm	80.74 ± 4.92	76.31 ± 11.75	**0.01**
Superior nasal GCL+IPL, μm	81.41 ± 5.48	76.51 ± 14.05	**< 0.01**
Inferior nasal GCL+IPL, μm	80.22 ± 5.93	74.58 ± 13.30	**0.01**
Inferior GCL+IPL, μm	78.41 ± 5.92	74.31 ± 12.44	**0.03**
Inferior temporal GCL +IPL, μm	80.07 ± 6.59	77.78 ± 16.06	0.12

Statistically significant values are in bold.

Comparisons with significance level $P < 0.05$ were considered statistically significant.

*It was analyzed with Mann-Whitney *U* test (Healthy vs. XFS).

GCL+IPL indicates ganglion cell layer and internal plexiform layer; OCT, optical coherence tomography; RNFLT, retinal nerve fiber layer thickness; XFS, exfoliation syndrome.

microvascular damage contributes to the pathogenesis of XFS and precedes significant GCL+IPL and RNFLT thinning.

While both decreased peripapillary RNFLT and macular GCC measurements have been observed in XFS eyes, it is difficult to predict whether vascular damage or RNFLT thinning begins first. The RPC network is a vascular plexus in the RNFL; the capillaries run along relatively long straight paths and are limited to the posterior pole, where they seem to be highly associated with superficial nerve fibers.[21,22] The pathogenesis of glaucoma and many retinal vascular diseases are thought to be closely related to the RPC network, as several functional and structural changes, such as Bjerrum scotoma, cottonwool spots, and frame-shaped retinal hemorrhages, match the distribution of this network.[23,24] While histopathologic studies have been performed in rhesus monkeys, cats, and human donor eyes to better elucidate the features of the RPC network, the evaluation of the vascular network *in vivo* was limited—even with the use of conventional fluorescein angiography.[22–24] The development of OCT-A has made it possible to evaluate the RPC network more precisely.

Previously, before the widespread use of OCT-A devices, Ocakoğlu et al[10] demonstrated reduced blood flow rates in the optic nerve head and peripapillary retina in patients with unilateral XFS. A recent meta-analysis of 225 XFS eyes and 208 healthy eyes found that RNFLT was significantly lower in XFS eyes.[25] Using OCT-A and OCT, Göker et al[26] observed that RPC VDs and RNFLTs in the peripapillary region were significantly lower in XFS eyes than in unaffected fellow or control eyes. In our study, RNFLT and peripapillary VDs were similar between the XFS and healthy groups. Prior studies have shown a progressive decrease in perfused capillary VDs from healthy eyes, to XFS eyes, to XFS glaucoma eyes. A direct correlation was also reported between peripapillary RNFLT and peripapillary VDs, as measured with AngioVue, in patients with POAG.[17,24] Comparing peripapillary AngioVue OCT-A parameters between patients with XFS glaucoma and their age-matched and glaucoma-stage-matched counterparts with POAG, Rebolleda et al[27] demonstrated that the former featured significantly lower VDs. The authors considered their findings to indicate that patients with XFS have relatively more severe vascular impairment.[24] Similarly, Suwan et al[17] demonstrated that peripapillary VD was more significantly decreased in patients with XFS

TABLE 3. Disc Parameters of the Groups Measured by OCT

	Healthy	XFS	*P**
Rim area, mm^2	1.25 ± 0.23	1.28 ± 0.23	0.42
Disc area, mm^2	1.74 ± 0.24	1.83 ± 0.36	0.72
Mean cupping/disc	0.56 ± 0.17	0.51 ± 0.15	0.58
Vertical cupping/disc	0.45 ± 0.15	0.51 ± 0.17	0.37
Cupping volume, mm^3	0.14 ± 0.16	0.17 ± 0.14	0.53

Comparisons with significance level $P < 0.05$ were considered statistically significant.

*It was analyzed with Mann-Whitney *U* test (Healthy vs. XFS).

OCT indicates optical coherence tomography; XFS, exfoliation syndrome.

TABLE 4. Peripapillary Vessel Density Measurements of Groups

	Healthy	XFS	*P**
WI-PPVD	47.45 ± 4.00	46.92 ± 3.54	0.52
IDDD	45.72 ± 5.17	45.07 ± 5.41	0.57
PPVD	50.26 ± 4.98	49.59 ± 3.83	0.49
SH-PPVD	50.51 ± 4.72	49.72 ± 4.16	0.43
IH-PPVD	50.01 ± 5.54	49.43 ± 3.78	0.58
S-PPVD	50.05 ± 6.37	48.79 ± 4.83	0.32
T-PPVD	50.85 ± 6.03	49.12 ± 7.97	0.32
I-PPVD	52.0 ± 5.87	51.08 ± 4.46	0.43
N-PPVD	50.56 ± 7.64	48.74 ± 8.02	0.30

Comparisons with significance level $P < 0.05$ were considered statistically significant.

*It was analyzed with Mann-Whitney *U* test (Healthy vs. XFS).

IDVD indicates inside disc vessel density; PPVD: peripapillary vessel density; IH-PPVD: inferior hemi peripapillary vessel density; I-PPVD: inferior quadrant peripapillary vessel density; N-PPVD: nasal quadrant peripapillary vessel density; SH-PPVD: superior hemi peripapillary vessel density; S-PPVD: superior quadrant peripapillary vessel density; T-PPVD: temporal quadrant peripapillary vessel density; WI-PPVD: whole image peripapillary vessel density; XFS: Exfoliation syndrome.

TABLE 5. Parafoveal Vessel Density Measurements of the Groups

	Healthy	XFS	*P**
WI-MVD	46.84 ± 3.78	45.38 ± 4.56	0.17
PFVD	48.34 ± 5.81	45.44 ± 5.81	**0.02**
SH-PFVD	48.43 ± 4.90	45.85 ± 6.26	**0.04**
IH-PFVD	48.21 ± 5.99	45.54 ± 6.01	**0.04**
S-PFVD	48.89 ± 5.55	47.11 ± 6.77	0.19
T-PFVD	48.53 ± 5.00	45.64 ± 7.37	**0.04**
I-PFVD	48.56 ± 6.15	46.41 ± 6.37	0.12
N-PFVD	47.49 ± 5.93	43.63 ± 6.98	**0.01**

Statistically significant values are in bold.

Comparisons with significance level $P < 0.05$ were considered statistically significant.

*It was analyzed with Mann-Whitney *U* test (Healthy vs. XFS).

IH-PFVD indicates inferior hemi parafoveal vessel density; I-PFVD, inferior parafoveal vessel density; N-PFVD, nasal parafoveal vessel density; PFVD, parafoveal vessel density; SH-PFVD, superior hemi parafoveal vessel density; S-PFVD, superior parafoveal vessel density; T-PFVD, temporal parafoveal vessel density; WI-MVD, whole image macular vessel density; XFS, Exfoliation syndrome.

TABLE 6. Correlation Analysis of GCL+IPL and Macular OCT-A Measurements in All Groups

	Healthy	XFS
Mean GCL+IPL/WI-MVD		
r	0.324	**0.432**
P	0.10	**< 0.01**
Mean GCL+IPL /PFVD		
r	0.195	**0.296**
P	0.33	**0.04**
Min GCL+IPL/WI-MVD		
r	0.366	**0.422**
P	0.06	**< 0.01**
Min GCL+IPL/PFVD		
r	0.283	**0.302**
P	0.15	**0.04**
SH-GCL+IPL/ SH-PFVD		
r	0.086	0.294
P	0.67	0.05
IH-GCL+IPL/IH-PFVD		
r	0.342	0.127
P	0.08	0.41

Statistically significant values are in bold.

Spearman correlation test was used. *P*: statistical difference, *r*: correlation coefficient.

GCL+IPL indicates ganglion cell layer and internal plexiform layer; IH-GCL+IPL, inferior hemi ganglion cell layer and internal plexiform layer; IH-PFVD, inferior hemi parafoveal vessel density; OCT-A, optical coherence tomography angiography; PFVD, parafoveal vessel density; SH-GCL+IPL, superior hemi ganglion cell layer and internal plexiform layer; SH-PFVD, superior hemi parafoveal vessel density; WI-MVD, whole image macular vessel density; XFS, exfoliation syndrome.

glaucoma compared with healthy controls and those with POAG or XFS patients; this finding was interpreted as quantitative evidence for microvascular disturbance in XFS. Park et al[28] attributed their finding, that peripapillary VD was lower in eyes with XFS glaucoma than in those with POAG, to ischemic damage caused by XFS material. The present study found that the detection of macular vascular changes in patients with XFS before their RNFLs and peripapillary VDs have deteriorated can support ischemic injury in the pathogenesis of XFS. Moreover, our findings support that XFS-associated vascular damage first affects the macular vessels.

Çınar and colleagues compared the flow and VD in the retina and choroid in XFS eyes, fellow eyes without XFS, and healthy eyes using OCTA; the total, parafoveal, and foveal flow and VD in the superficial capillary plexus were found to be the lowest in XFS eyes. The study further revealed that superficial retinal blood flow and VD parameters were lower in XFS eyes than in healthy eyes, while deep blood flow and VD parameters were unaffected by XFS. In addition, they observed the enlargement of the foveal avascular zone in XFS eyes. The authors interpreted these findings as evidence of XFS-related vascular pathology.[29] Similarly, our investigation found that superficial parafoveal VD parameters were significantly lower in the XFS group. We did not evaluate deep VD parameters because the superficial capillary plexus is mainly responsible for the vascular supply of ganglion cells, which are found in superficial layers. The effects of XFS on retinal vascular parameters were investigated before using alternative techniques. Choroidal thinning, which suggests a reduction in choroidal blood flow, was previously reported in XFS eyes.[29–31] Yüksel et al[32] have reported a significant reduction in retinal blood flow in XFS eyes measured with color Doppler ultrasound. The thinning of the ganglion cell layer and superficial retinal layers in XFS eyes has been previously reported in the literature, and the minimum GCL +IPL has been shown to be the most accurate parameter for diagnosing glaucoma.[21,33] As the susceptibility of retinal ganglion cells to glaucomatous damage differs across regions, the minimum GCL+IPL thickness is a more sensitive diagnostic parameter than the average or sectoral GCL+IPL thickness measurements.[33,34] We found a lower minimum GCL+IPL thickness in patients with XFS than in healthy controls, but there was no difference in the mean GCL+IPL thickness between the two groups. When we examined the GCL+IPL sectorally, we found thinning in all sectoral areas except the temporal sectors. Our findings of reduced VD in superficial macular layers may indicate an underlying vascular pathology. While GCL+IPL reduction was not obvious, we detected VD reduction in the macular area.

To the best of our knowledge, this study is the first to investigate both peripapillary and macular OCT-A parameters in XFS eyes. The RNFLT values of the XFS group in our study were similar to those of the healthy group. Investigating structural OCT changes in XFS patients without glaucoma, Eltutar and colleagues found the thicknesses of the macular ganglion cell complex and nerve fiber layer to be significantly lower in XFS eyes than in healthy eyes. This difference was considered to indicate that the macular area could be affected independently by the increase in IOP induced by XFS syndrome.[21] The present study included patients with no defects in the peripapillary RNFL or in the GCA. We found significantly lower superficial macular VDs in XFS eyes than in healthy eyes. The fact that the most sectoral GCL +IPL and the minimum GCL+IPL thickness is decreased in patients with XFS relative to healthy controls further supports our findings. As the superficial vessels are primarily responsible for the nourishment of superficial macular layers, our results can explain those obtained by Eltutar et al.[21] While the pathogenesis of XFS and its progression to glaucoma remains unclear, we believe that our findings provide insight into XFS pathogenesis by demonstrating XFS-induced microvascular effects with OCT-A.

This study was limited by its cross-sectional design. A longitudinal study could have demonstrated the effects of XFS progression, especially on peripapillary VD parameters, and we would have shown if the reduction in VD becomes significant with the progression of XFS. Our study was further limited by its small sample size. However, we consider such limitation to be partially offset by its being the first to compare both macular and peripapillary VD parameters in XFS and healthy controls and to thus elucidate the effect of vascular pathology in patients with XFS.

In conclusion, although the RNFLT values of healthy controls and XFS patients were similar, we demonstrated that superficial macular VDs were significantly lower in the XFS group than in the healthy group. In addition, while the mean GCL+IPL was found to be similar between the two groups, the minimum GCL+IPL and sectoral GCL+IPL thicknesses were lower in the XFS group. Our findings suggest that XFS causes vascular damage and decreased VDs. These effects may induce ischemia. This possibility may guide future research into the unclear mechanisms underlying XFS-related glaucomatous damage.

ACKNOWLEDGMENTS

The authors would like to thank Editage (http://www.editage.com) for English language editing.

REFERENCES

1. Aboobakar IF, Johnson WM, Stamer WD, et al. Major review: exfoliation syndrome; advances in disease genetics, molecular biology, and epidemiology. *Exp Eye Res*. 2017;154:88–103.
2. Terracciano L, Cennamo M, Favuzza E, et al. An in vivo confocal microscopy study of corneal changes in pseudoexfoliation syndrome. *Eur J Ophthalmol*. 2019;29:555–560.
3. Ritch R, Schlotzer-Schrehardt U. Exfoliation syndrome. *Surv Ophthalmol*. 2001;45:265–315.
4. Naumann GO, Schlotzer-Schrehardt U, Kuchle M. Pseudoexfoliation syndrome for the comprehensive ophthalmologist. Intraocular and systemic manifestations. *Ophthalmology*. 1998;105:951–968.
5. Anastasopoulos E, Founti P, Topouzis F. Update on pseudoexfoliation syndrome pathogenesis and associations with intraocular pressure, glaucoma and systemic diseases. *Curr Opin Ophthalmol*. 2015;26:82–89.
6. Ritch R. Ocular and systemic manifestations of exfoliation syndrome. *J Glaucoma*. 2014;23(suppl 1):S1–S8.
7. Yuksel N, Anik Y, Kilic A, et al. Cerebrovascular blood flow velocities in pseudoexfoliation. *Graefes Arch Clin Exp Ophthalmol*. 2006;244:316–321.
8. Grodum K, Heijl A, Bengtsson B. Risk of glaucoma in ocular hypertension with and without pseudoexfoliation. *Ophthalmology*. 2005;112:386–390.
9. Citirik M, Acaroglu G, Batman C, et al. A possible link between the pseudoexfoliation syndrome and coronary artery disease. *Eye (Lond)*. 2007;21:11–15.
10. Ocakoglu O, Koyluoglu N, Kayiran A, et al. Microvascular blood flow of the optic nerve head and peripapillary retina in unilateral exfoliation syndrome. *Acta Ophthalmol Scand*. 2004; 82:49–53.
11. Khalil AK, Kubota T, Tawara A, et al. Early changes in iris blood vessels in exfoliation syndrome. *Curr Eye Res*. 1998;17: 1124–1134.
12. Harju M, Kurvinen L, Saari J, et al. Blood flow in the peripapillary retina in exfoliation glaucoma. *Clin Exp Ophthalmol*. 2008;36:738–743.
13. Ringvold A. Light and electron microscopy of the wall of iris vessels in eyes with and without exfoliation syndrome (pseudoexfoliation of the lens capsule). *Virchows Arch A Pathol Pathol Anat*. 1970;349:1–9.
14. Asano N, Schlotzer-Schrehardt U, Naumann GO. A histopathologic study of iris changes in pseudoexfoliation syndrome. *Ophthalmology*. 1995;102:1279–1290.
15. Mansouri K. Optical coherence tomography angiography and glaucoma: searching for the missing link. *Expert Rev Med Devices*. 2016;13:879–880.
16. Jia Y, Morrison JC, Tokayer J, et al. Quantitative OCT angiography of optic nerve head blood flow. *Biomed Opt Express*. 2012;3:3127–3137.
17. Suwan Y, Geyman LS, Fard MA, et al. Peripapillary perfused capillary density in exfoliation syndrome and exfoliation glaucoma versus POAG and healthy controls: an OCTA study. *Asia Pac J Ophthalmol (Phila)*. 2018;7:84–89.
18. Scripsema NK, Garcia PM, Bavier RD, et al. Optical coherence tomography angiography analysis of perfused peripapillary capillaries in primary open-angle glaucoma and normal-tension glaucoma. *Invest Ophthalmol Vis Sci*. 2016;57:OCT611–OCT620.
19. Nesper PL, Roberts PK, Onishi AC, et al. Quantifying microvascular abnormalities with increasing severity of diabetic retinopathy using optical coherence tomography angiography. *Invest Ophthalmol Vis Sci*. 2017;58:BIO307–BIO315.
20. Xu X, Xiao H, Guo X, et al. Diagnostic ability of macular ganglion cell–inner plexiform layer thickness in glaucoma suspects. *Medicine*. 2017;96:e9182.
21. Eltutar K, Acar F, Kayaarasi Ozturker Z, et al. Structural changes in pseudoexfoliation syndrome evaluated with spectral domain optical coherence tomography. *Curr Eye Res*. 2016;41: 513–520.
22. Henkind P. Radial peripapillary capillaries of the retina. I. Anatomy: human and comparative. *Br J Ophthalmol*. 1967;51: 115–123.
23. Alterman M, Henkind P. Radial peripapillary capillaries of the retina. II. Possible role in Bjerrum scotoma. *Br J Ophthalmol*. 1968;52:26–31.
24. Yu PK, Cringle SJ, Yu DY. Correlation between the radial peripapillary capillaries and the retinal nerve fibre layer in the normal human retina. *Exp Eye Res*. 2014;129:83–92.
25. Yu JG, Huang Q, Zhou XF, et al. Retinal nerve fiber layer thickness changes in the pseudoexfoliation syndrome: a meta-analysis of case-control studies. *Ophthalmic Res*. 2018;59: 14–23.
26. Goker YS, Kiziltoprak H. Quantitative analysis of radial peripapillary capillary plexuses in patients with clinically unilateral pseudoexfoliation syndrome. *Graefes Arch Clin Exp Ophthalmol*. 2020;258:1217–1225.
27. Rebolleda G, Pérez-Sarriegui A, De Juan V, et al. A comparison of two optical coherence tomography-angiography devices in pseudoexfoliation glaucoma versus primary open-angle glaucoma and healthy subjects. *Eur J Ophthalmol*. 2019;29: 636–644.
28. Park JH, Yoo C, Girard MJA, et al. Peripapillary vessel density in glaucomatous eyes: comparison between pseudoexfoliation glaucoma and primary open-angle glaucoma. *J Glaucoma*. 2018;27:1009–1016.
29. Cinar E, Yuce B, Aslan F. Retinal and choroidal vascular changes in eyes with pseudoexfoliation syndrome: a comparative study using optical coherence tomography angiography. *Balkan Med J*. 2019;37:9–14.
30. Demircan S, Yilmaz U, Kucuk E, et al. The effect of pseudoexfoliation syndrome on the retinal nerve fiber layer and choroid thickness. *Semin Ophthalmol*. 2017;32:341–347.
31. Eroglu FC, Asena L, Simsek C, et al. Evaluation of choroidal thickness using enhanced depth imaging by spectral-domain optical coherence tomography in patients with pseudoexfoliation syndrome. *Eye (Lond)*. 2015;29:791–796.
32. Yuksel N, Karabas VL, Arslan A, et al. Ocular hemodynamics in pseudoexfoliation syndrome and pseudoexfoliation glaucoma. *Ophthalmology*. 2001;108:1043–1049.
33. Jung JH, Seo JH, Kang MS, et al. Comparison of glaucoma diagnostic ability of ganglion cell-inner plexiform layer according to the range around the fovea. *BMC Ophthalmol*. 2019; 19:270.
34. Jeoung JW, Choi YJ, Park KH, et al. Macular ganglion cell imaging study: Glaucoma diagnostic accuracy of spectral-domain optical coherence tomography. *Invest Ophthalmol Vis Sci*. 2013;54:4422–4429.